Rehabilitation of biomechanics (336506)

Final project

Dmitry Rudman – 333814283

Oren Maya – 039680194

01.09.2020

Part 1 – Gait analysis

1. Introduction

In order to perform gate analysis, we used marker-based motion capture system. In marker-based techniques, video-based optoelectronic systems are used, when retro-reflective markers are attached on the human body.

Cameras - Each camera records the subject, whose motion is to be captured. The infrared lights form a “donut” shape around the lens. As the subject moves through the capture volume, infrared light is reflected back into the camera lens and strikes a light sensitive plate creating a video signal.

Markers - The subject has a number of reflective markers attached to their body, in well-defined positions. They reflect light straight back into the camera where they pass through a filter that allows light of only one particular wavelength (infrared) to be focused on the cameras sensitive plate.

Force plates - fixed in the ground and they record the force between the ground and the plantar surface of the foot. Force plates provide a three-dimensional description of the ground reaction force. The output signals show three components of the force (vertical, lateral and fore-aft), two coordinates of the center of pressure, and the moments about the vertical axis.

Datatype

We’ve collected data from experimental system which includes markers tracking and data from the force plates for static and dynamic parts. The software extracted the data according to biomechanical conventions.

Measurement errors

- Instrumental errors: these errors stem from the results of both instrumental noise and volume calibration inaccuracies. The instrumental noise can be reduced by low pass filtering, while the volume calibration inaccuracies depend on the inadequate number of cameras and the volume calibration algorithm chosen for the application.
- Soft tissue artefacts: the markers captured by the cameras can be directly attached to the skin or arranged in clusters and positioned with fixtures over a body segment and their movements cause errors. Since this error has the same frequency content as the bone movement, there is no way of distinguishing the artefact from the actual bone movement by using a filter. It is possible to reduce its effect by choosing marker locations so that the relative displacement is minimized. Secondly, mathematical operators can be used to estimate position and orientation of the bone from skin marker.
- Anatomical landmark misplacement: may result in wrong clinical interpretations of the estimation.

Calibration

Calibration allows the system to define the capture volume and the relative positions and orientations of cameras. This information is then used with the data from each camera to create the three-dimensional motion process. ***Static calibration*** is used to set the origin and the direction of the axes.

2. Data pre-processing

We choose to interpolate the data to put numbers instead of missing values. To do this we start with finding all NaN values (creating vector which consists of ones at indexes with NaN, and zeroes for any other value). Then we verify that NaN values are not at the end points, if they are – we change an end point to the nearest value. At the end we interpolate the data to the original length with interp1 interpolation function.

3. Simulation using figure stick

All frames were saved to a video, the video looks like realistic walking

4. Gait cycle

a) The gait cycle starting point – Heel Strike, described by the CM of the body being in the lowest point and minimal vertical position of the heel. So, we will look for minimal z values of the ankle (LANK and RANK). To find local minimums we use findpeaks function.

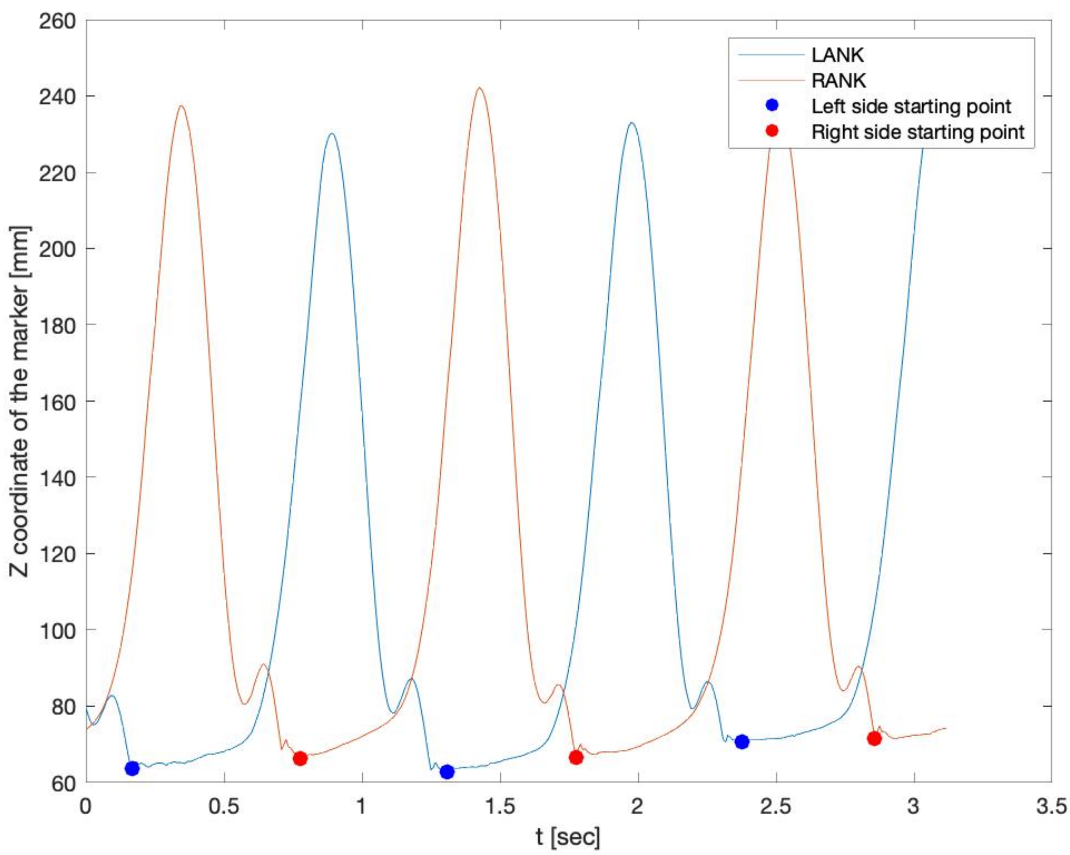

b) Plotting the average data of the flexion, adduction, and rotation angles of the hip, knee, and ankle of the left and right side with respect to the gait percentage. After splitting the data to the gate cycles, interpolation and averaging, we've got:

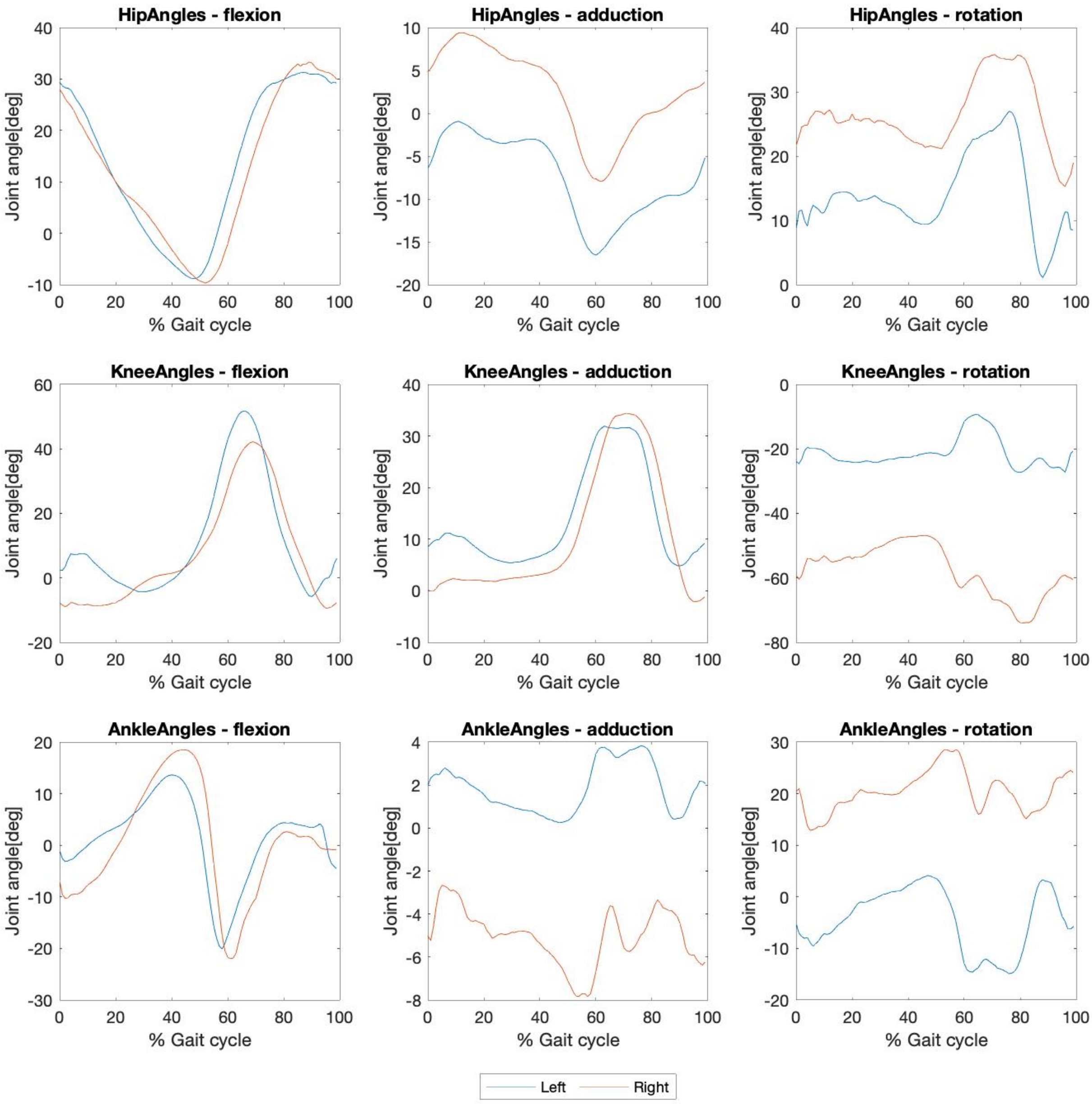

c) Comparing our results with the literature (two sources [1], [2]) :

First source, describes flexion during the gait cycle for hip, knee and ankle:

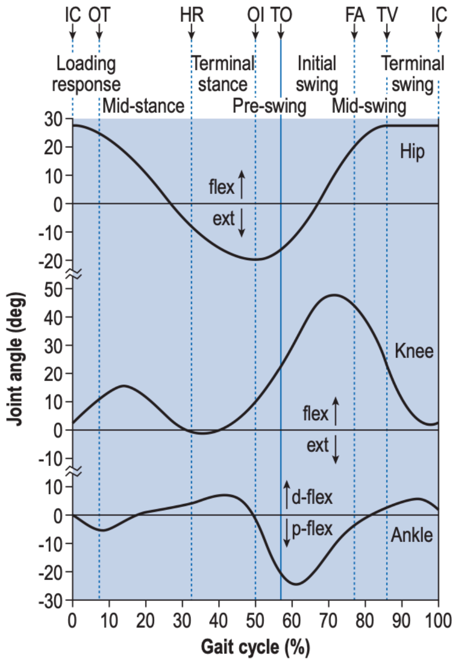

Second source, here we found graphs for adduction and rotation (only normal range is relevant for us)

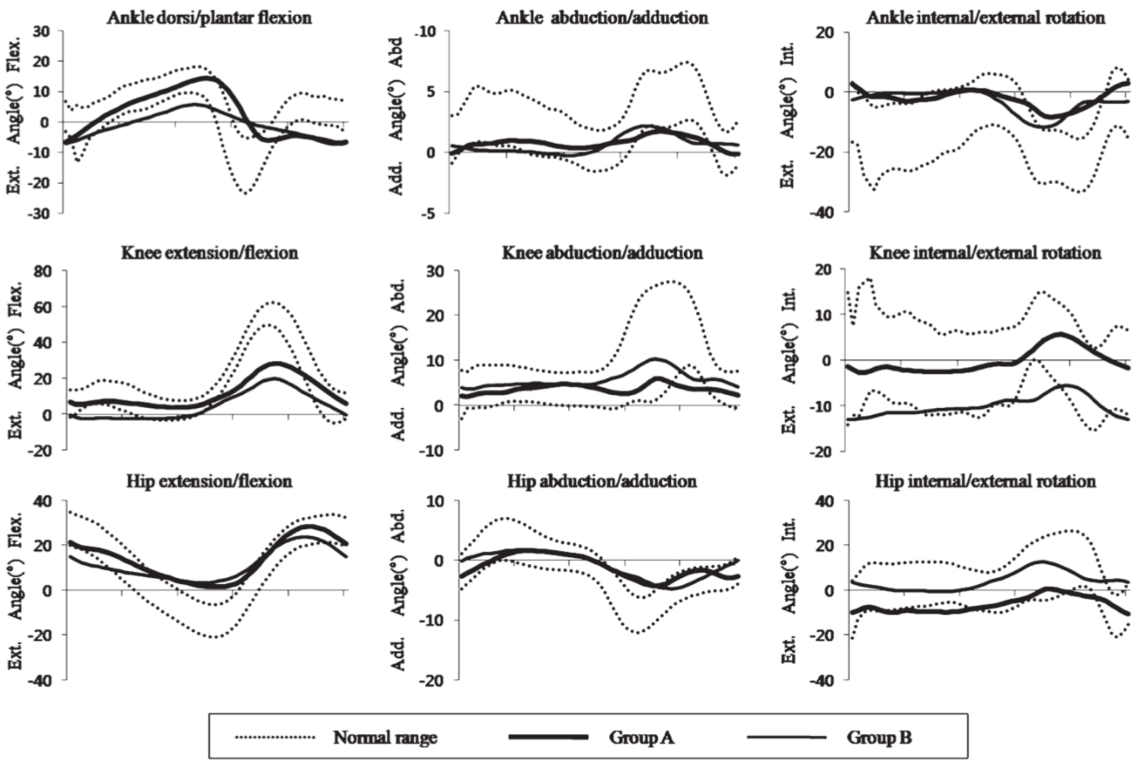

After comparing with the literature, we can conclude that we saw standard gait cycle of healthy individual.

5. Internal Forces and Moments Estimation

a) GRF and GRM for right and left legs:

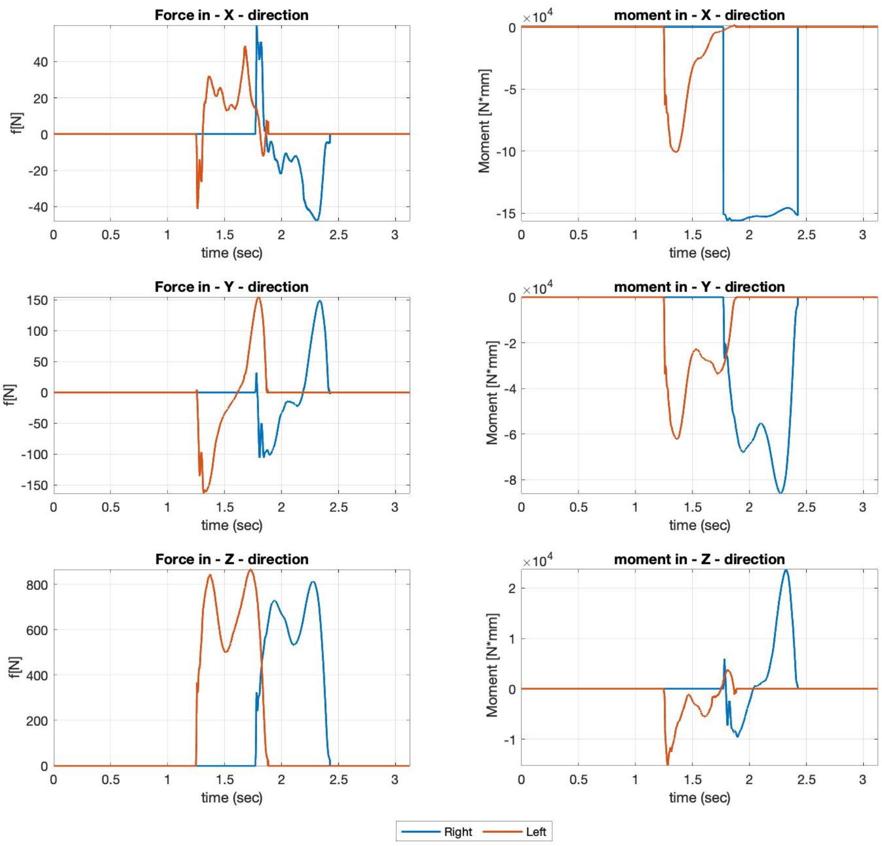

b) Comparing to the literature [3]:

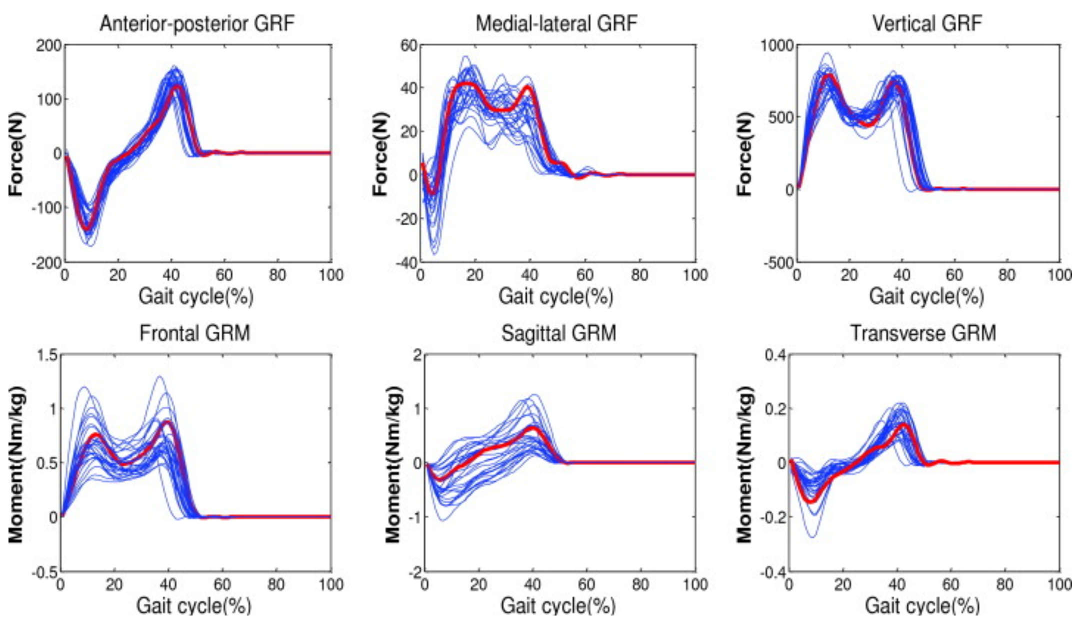

After comparing to the literature, we can conclude that there is a little difference when we compare medial-lateral and anterior-posterior GRM, it can be explained by gait features which are unique for every person.

c) Downsampling

Visualizing the process of downsampling shows that the data didn't change significantly (on example of the GRF of the right leg, similar for all other)

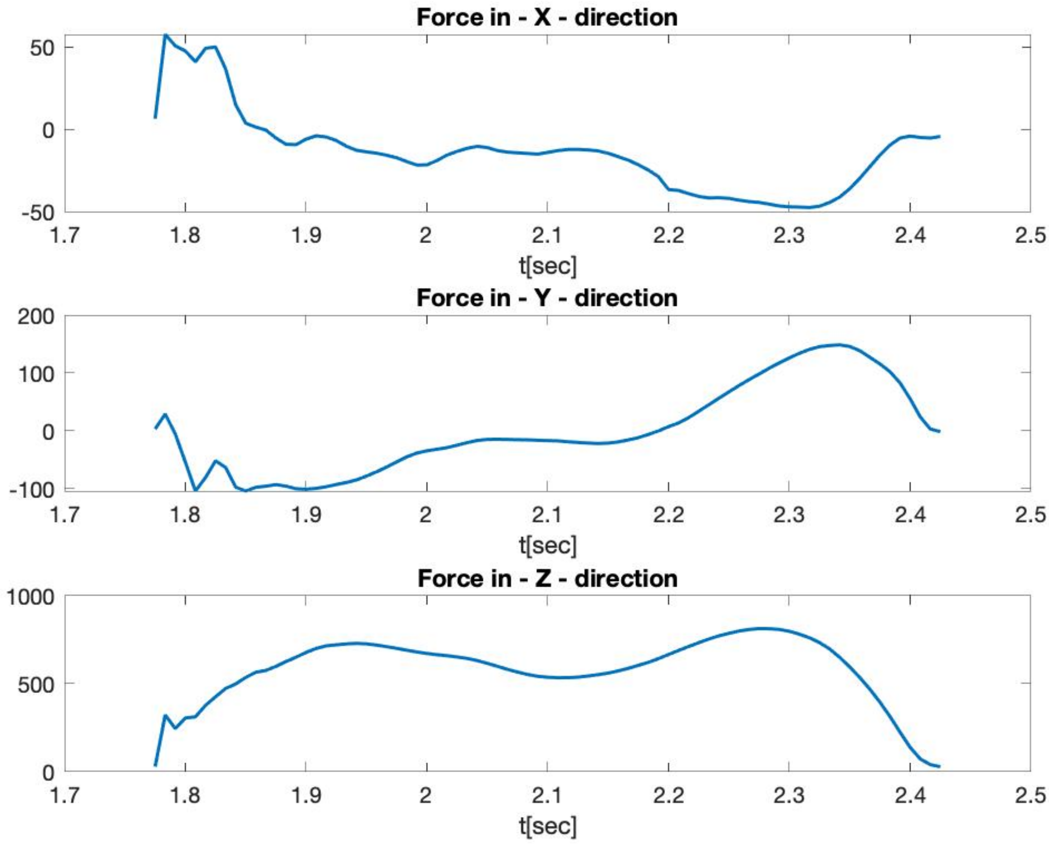

d+e) In order to calculate the internal forces and moments using GRF we use a link segment method, as we saw in the tutorial:

$$i = 1,\ldots,N \ segments,$$
$$i = 0 \rightarrow human/anatomical \ coordinates,$$
$$i = N+1 \rightarrow Lab \ coordinates:$$

$$\left(\underline{r}_{cm,i}\right)_{N+1} \xrightarrow{eq.(1)} \left(\underline{a}_{cm,i}\right)_{N+1}$$
$$\left\{\left(\underline{a}_{cm,i}\right)_{N+1}, \left(\underline{f}_{i+1}\right)_{N+1}, m_i\right\} \xrightarrow{eq.(2)} \left(\underline{f}_i\right)_{N+1}$$
$$\left(\underline{f}_i\right)_{N+1} \xrightarrow{R_i^{N+1}} \boxed{\left(\underline{f}_i\right)_i}$$
$$R_{i-1}^i \xrightarrow{eq.(3)} \left(\underline{\omega}_i\right)_i$$
$$\left\{R_{i-1}^i, \left(\underline{\omega}_i\right)_i\right\} \xrightarrow{eq.(4)} \left(\underline{\alpha}_i\right)_i$$
$$\left\{\begin{matrix} R_i^{i+1}, \left(\underline{\omega}_i\right)_i, \left(\underline{\alpha}_i\right)_i, \underline{\underline{I_i}} \\ \left(\underline{f}_{i+1}\right)_{i+1}, \left(\underline{\tau}_{i+1}\right)_{i+1} \end{matrix}\right\} \xrightarrow{eq.(5)} \boxed{\left(\underline{\tau}_i\right)_i}$$

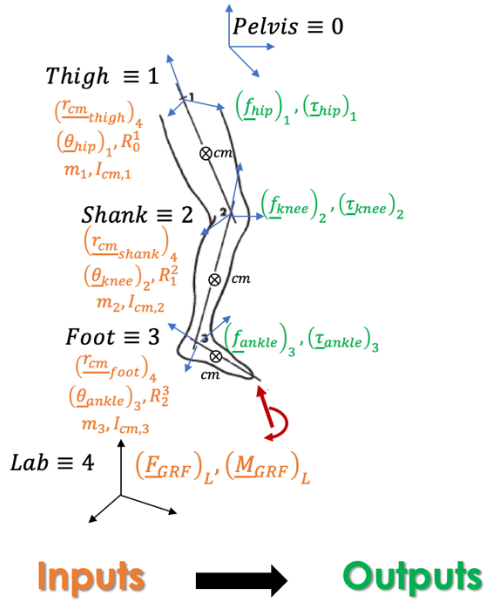

$$\boxed{(1): \left(\underline{a}_{cm,i}\right)_{Lab} = \left(\ddot{\underline{r}}_{cm,i}\right)_{Lab} = \begin{bmatrix} \ddot{r}_{cm,x,i} & \ddot{r}_{cm,y,i} & \ddot{r}_{cm,z,i} \end{bmatrix}_{Lab}^T}$$

$$\boxed{(2): \left(\underline{f}_i\right)_{Lab} = \left(\underline{f}_{i+1}\right)_{Lab} + m_i \cdot \left(\underline{a}_{cm,i}\right)_{Lab} - m_i \left(\underline{g}\right)_{Lab}}$$

$$\boxed{(3): \left[\left(\omega_i\right)_i\right]_\times = \left(R_{i-1}^i\right)^T \dot{R}_{i-1}^i}$$

$$\boxed{(4): \left[\left(\alpha_i\right)_i\right]_\times = \left(R_{i-1}^i\right)^T \ddot{R}_{i-1}^i - \left(\left[\left(\omega_i\right)_i\right]_\times\right)^2}$$

$$\boxed{\begin{aligned}(5): \left(\underline{\tau}_i\right)_i = {} & R_i^{i+1} \cdot \left(\underline{\tau}_{i+1}\right)_{i+1} - \left(\underline{f}_i\right)_i \times \left(\underline{r}_{cm,i}\right)_i + \left(R_i^{i+1} \cdot \left(\underline{f}_{i+1}\right)_{i+1}\right) \times \left(\underline{r}_{end \rightarrow cm,i}\right)_i + \\ & + \underline{\underline{I_{cm,i}}} \cdot \left(\underline{\alpha}_i\right)_i + \left(\underline{\omega}_i\right)_i \times \underline{\underline{I_{cm,i}}} \cdot \left(\underline{\omega}_i\right)_i = \end{aligned}}$$

f) For the width of the window of 2, after implementing the rotation matrix method, we've got:

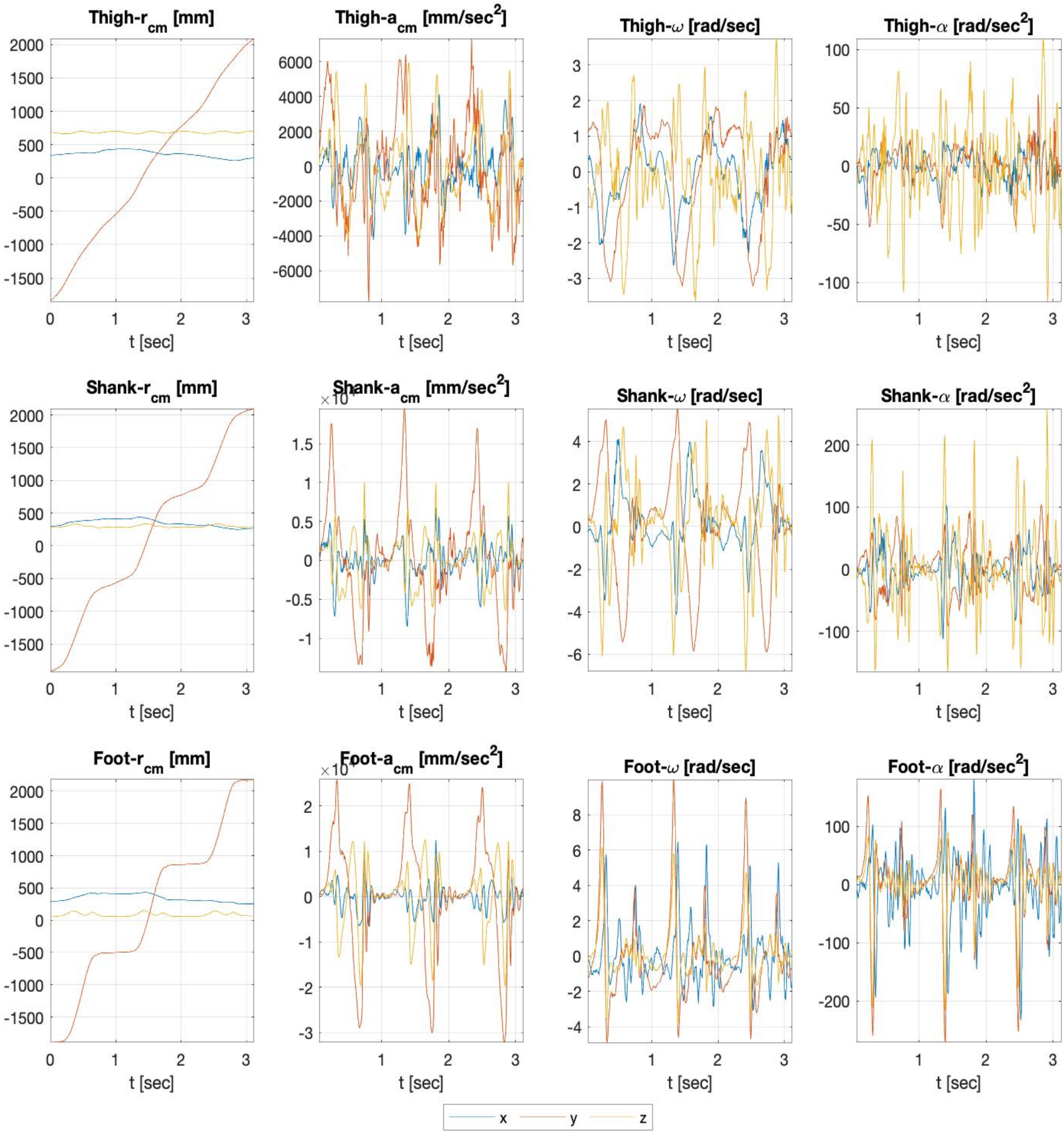

g) Internal forces and moment at the segment coordinate system for the time-points when the subject's right leg is one the force plate:

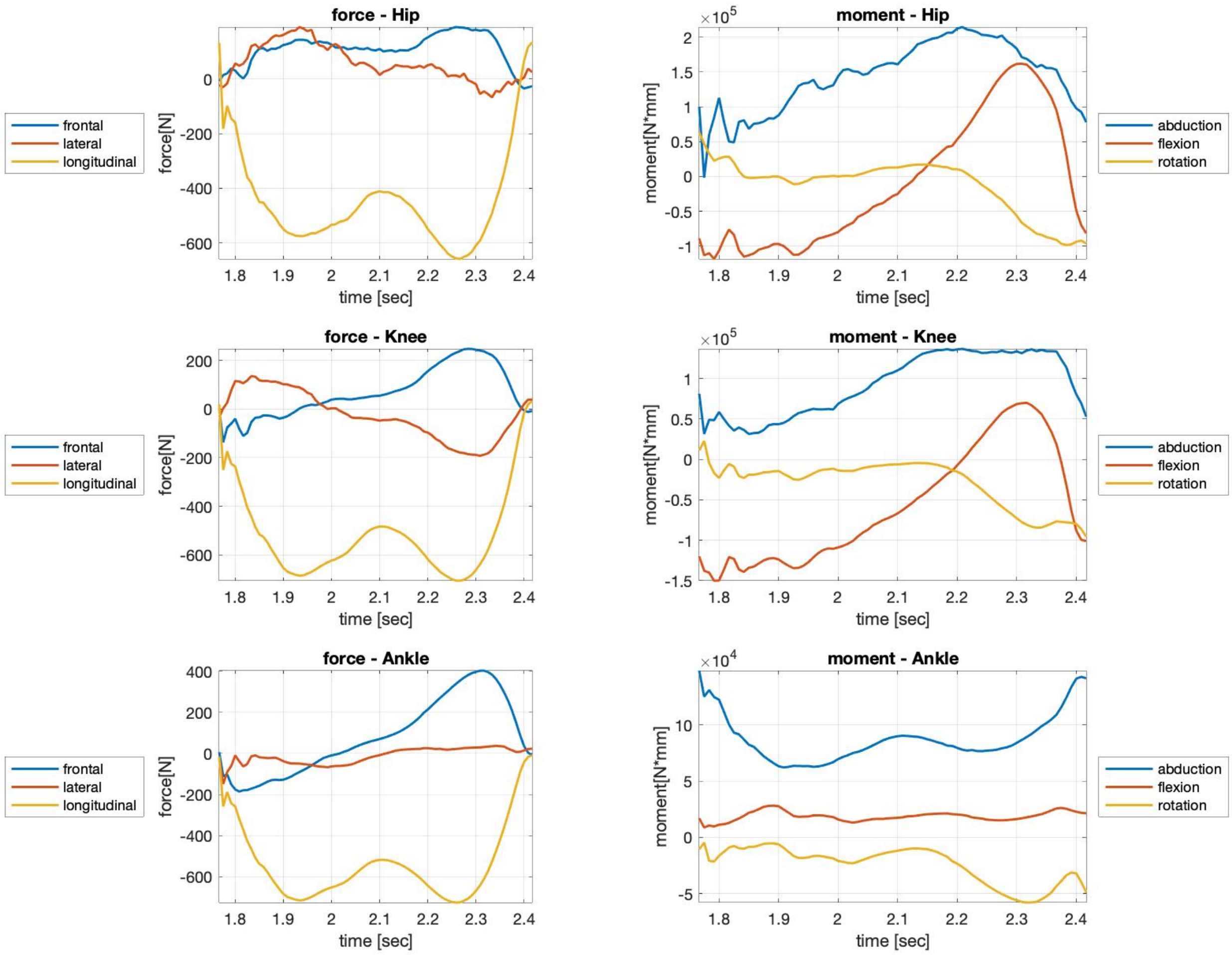

e) Comparing to the literature.
To verify our results, we found the reaction force components of the ankle in 3 planes [2], our results are very similar to the literature, as we expected. We can assume that other results are correct too.

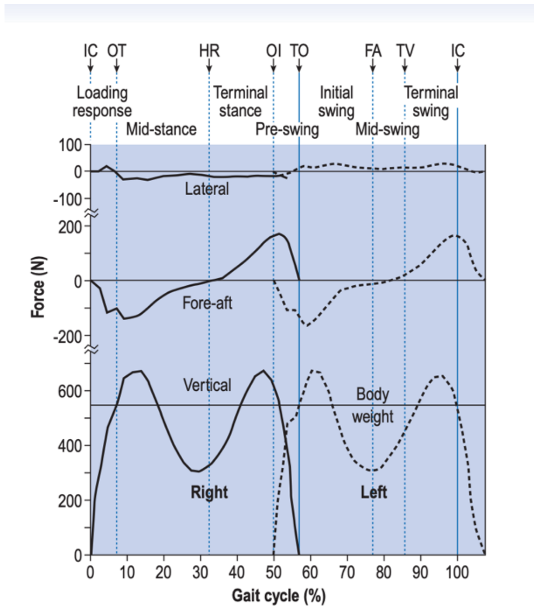

Part 2 – GRF and COP during split-belt adaptation

Q1.

a) Data was filtered with 4-th order Butterworth filter

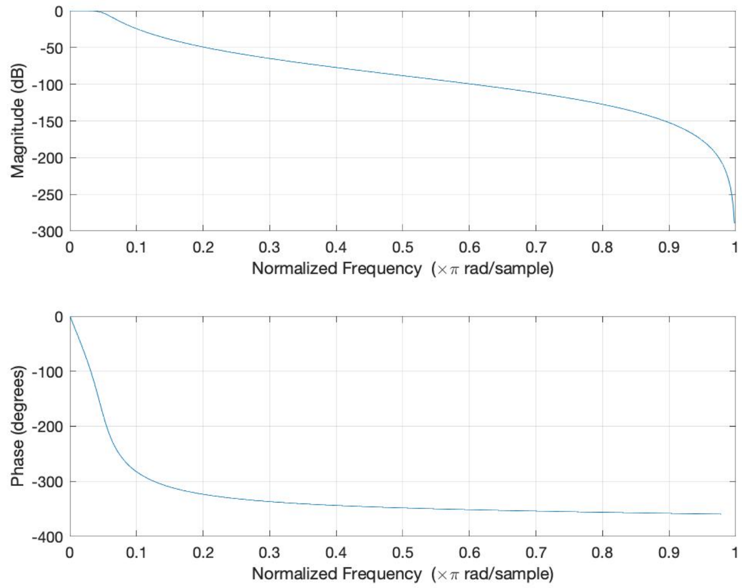

b)

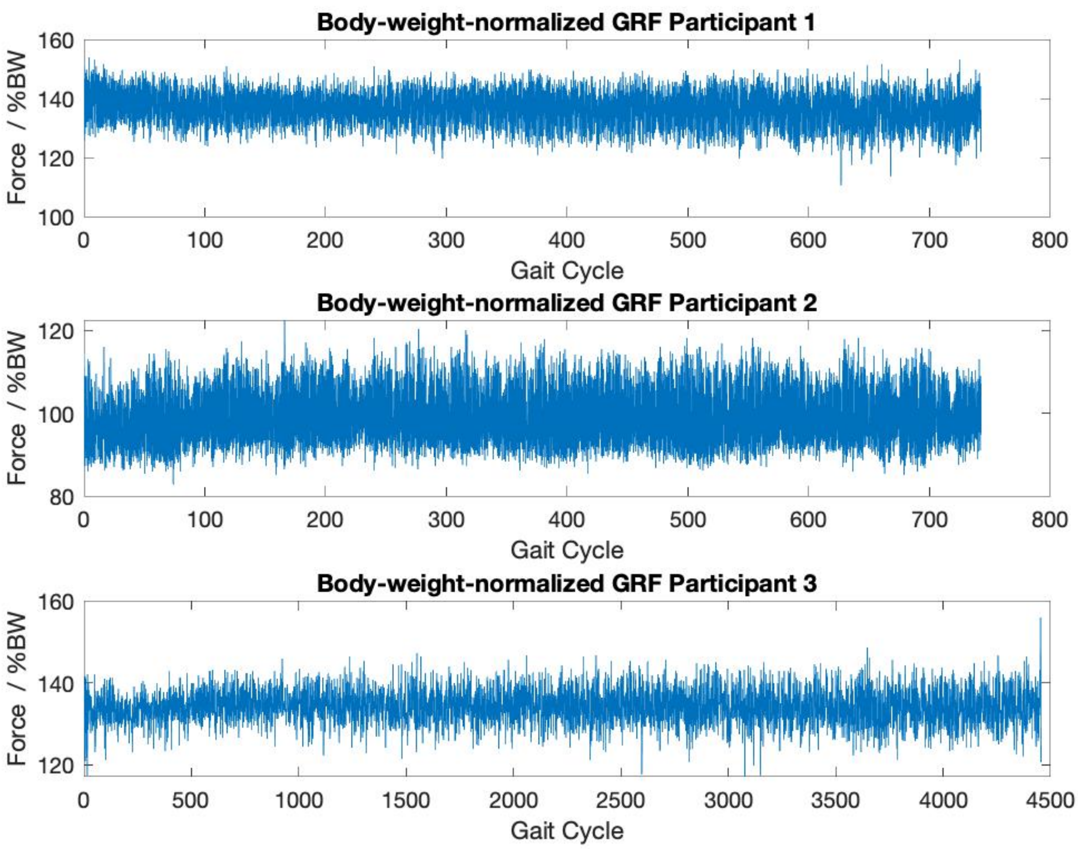

c+d) Heel Strike is the beginning of the cycle, Toe Off can be found around 60% of the cycle

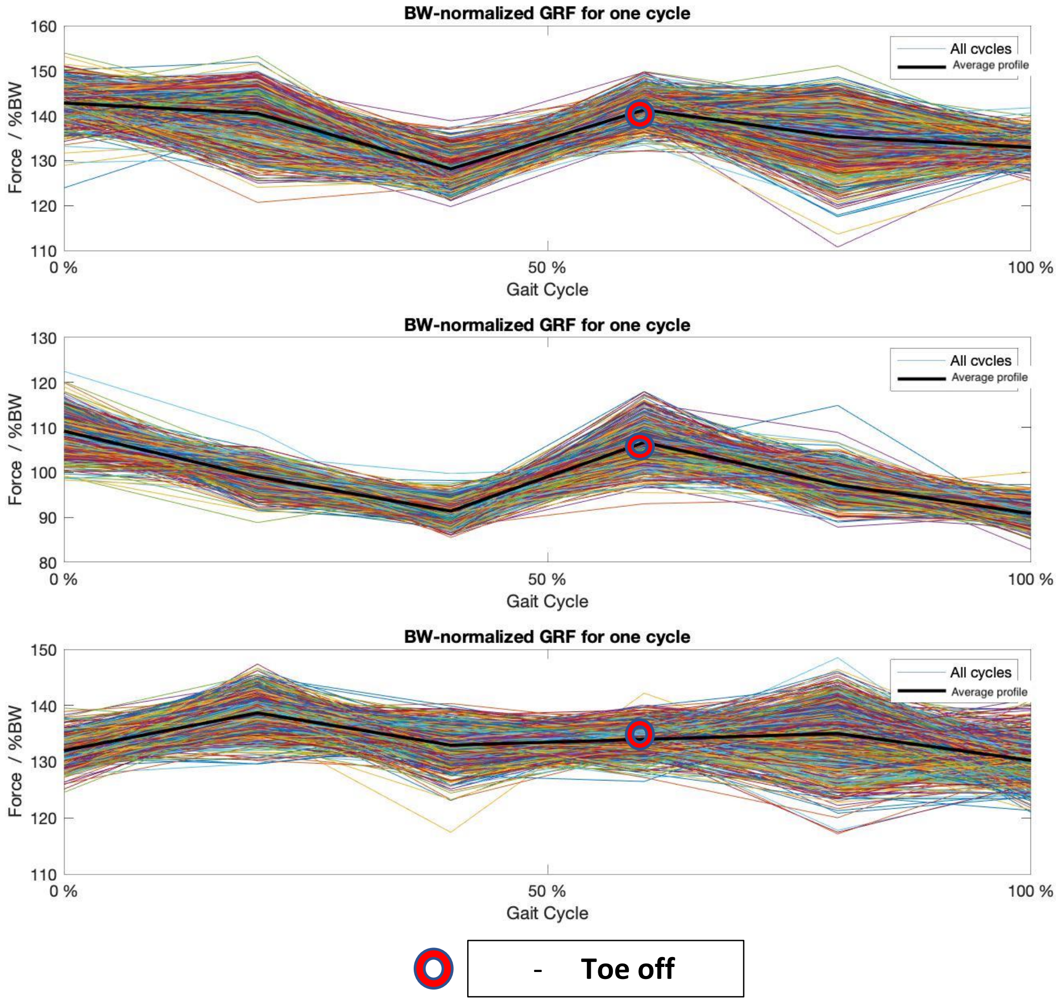

Q2

a+b)

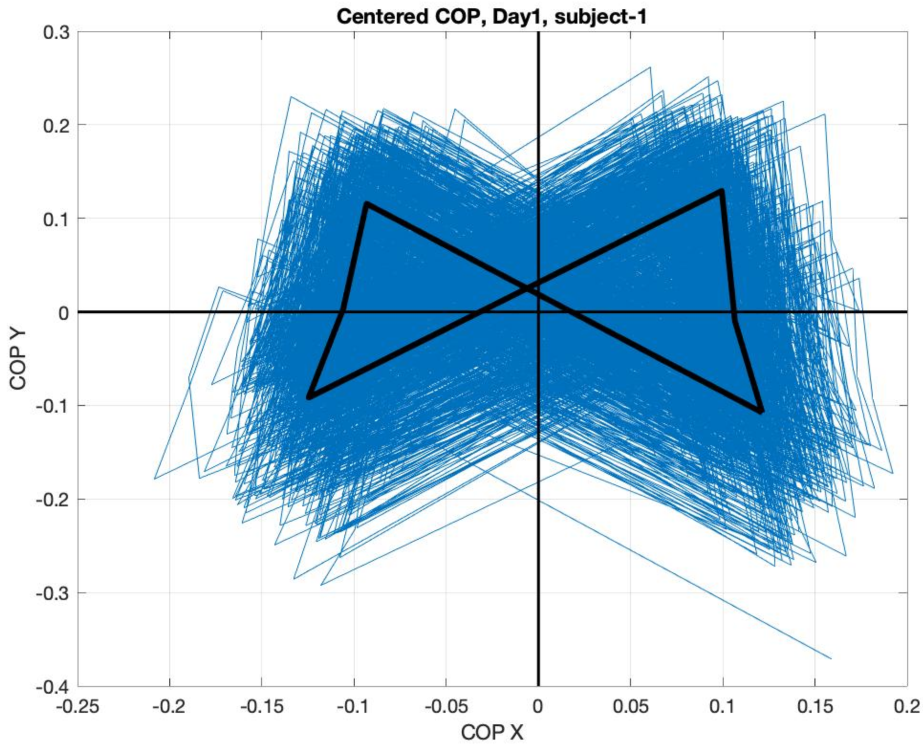

Centered COP, Day1, subject-1
COP Y
COP X
0.3
0.2
0.1
0
-0.1
-0.2
-0.3
-0.4
-0.25
-0.2
-0.15
-0.1
-0.05
0
0.05
0.1
0.15
0.2

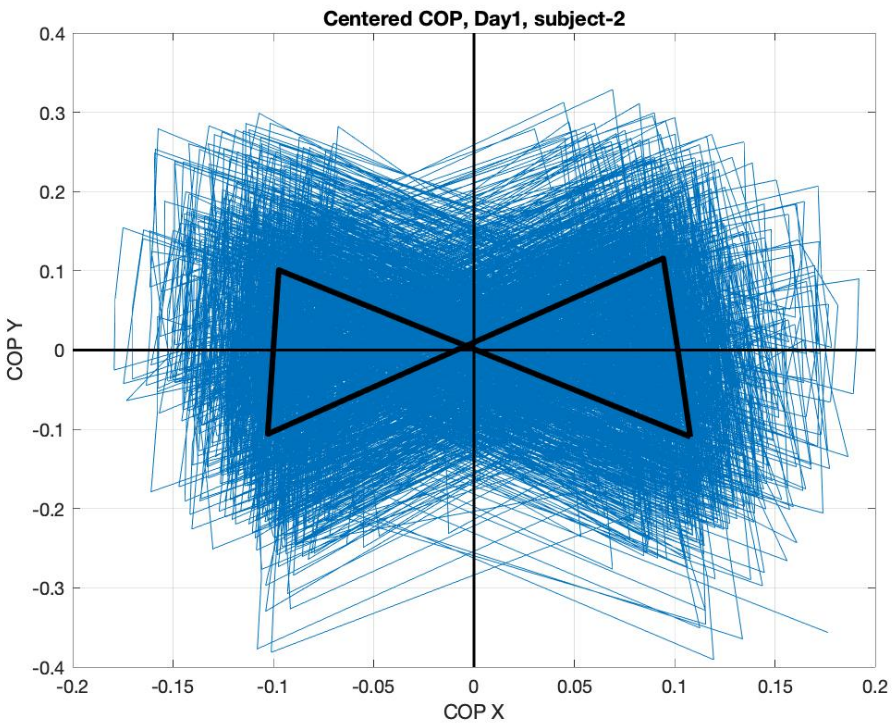

Centered COP, Day1, subject-2
COP Y
COP X
0.4
0.3
0.2
0.1
0
-0.1
-0.2
-0.3
-0.4
-0.2
-0.15
-0.1
-0.05
0
0.05
0.1
0.15
0.2

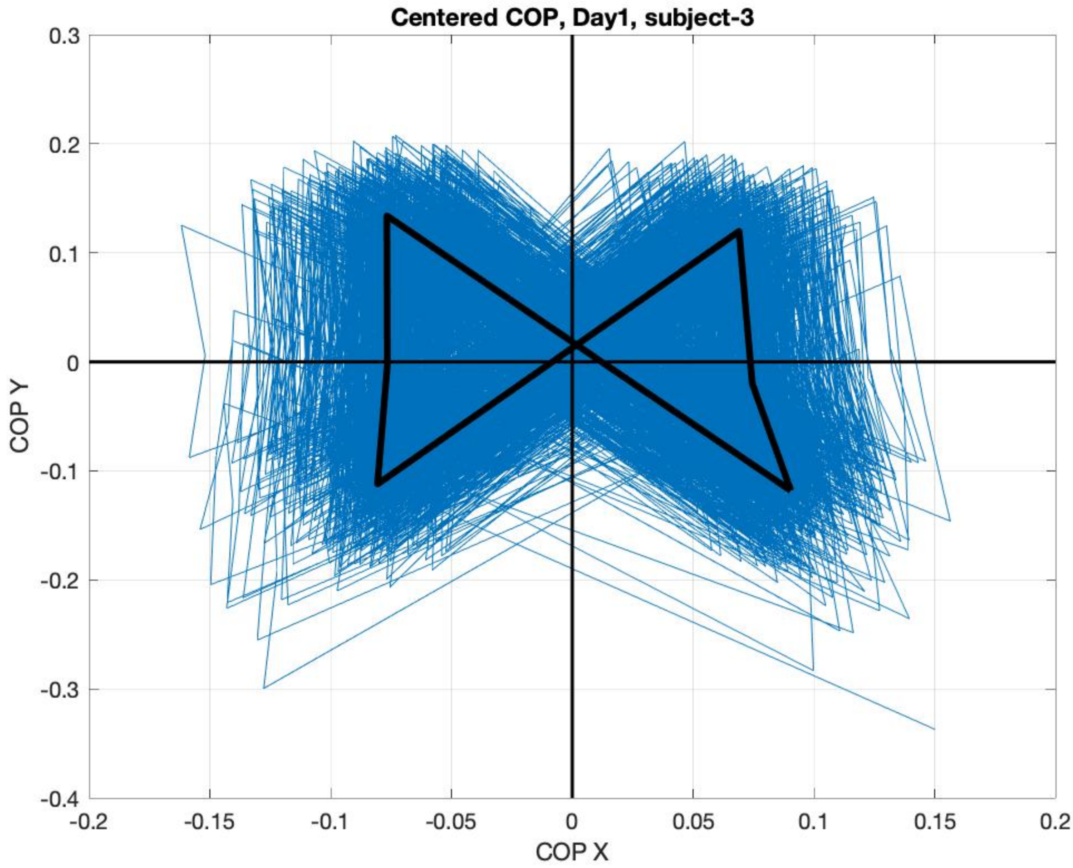

Centered COP, Day1, subject-3
0.3
0.2
0.1
0
-0.1
-0.2
-0.3
-0.4
COP Y
-0.2
-0.15
-0.1
-0.05
0
0.05
0.1
0.15
0.2
COP X

c) Day 2

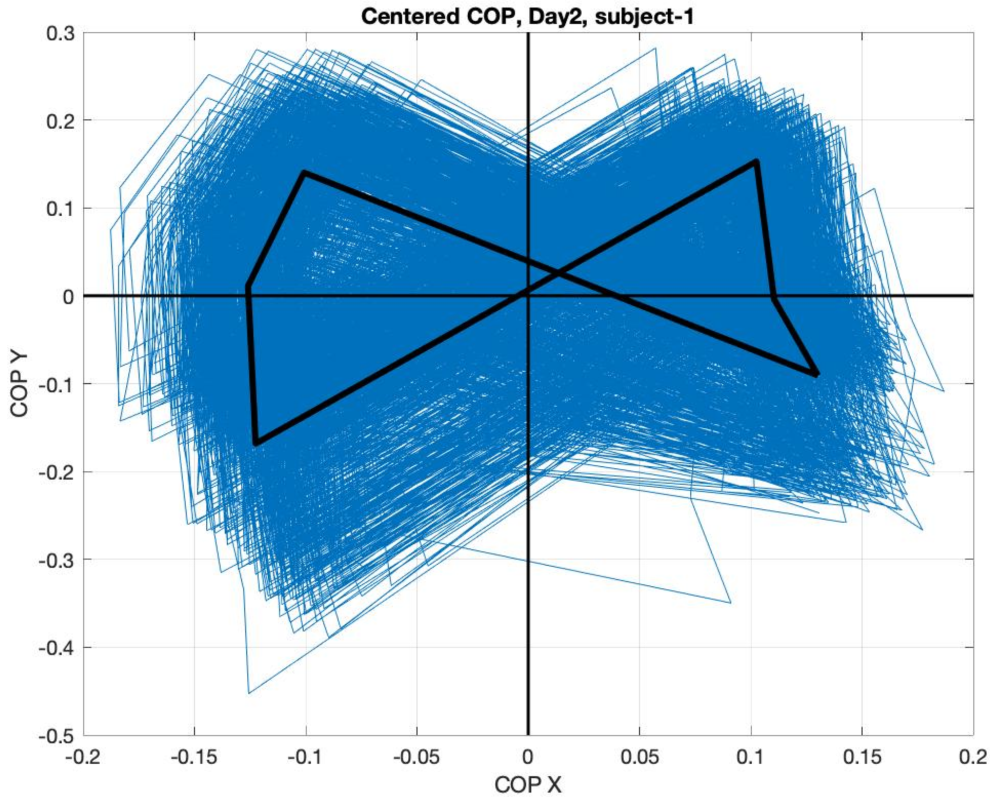
Centered COP, Day2, subject-1
0.3
0.2
0.1
0
-0.1
-0.2
-0.3
-0.4
-0.5
COP Y
-0.2
-0.15
-0.1
-0.05
0
0.05
0.1
0.15
0.2
COP X

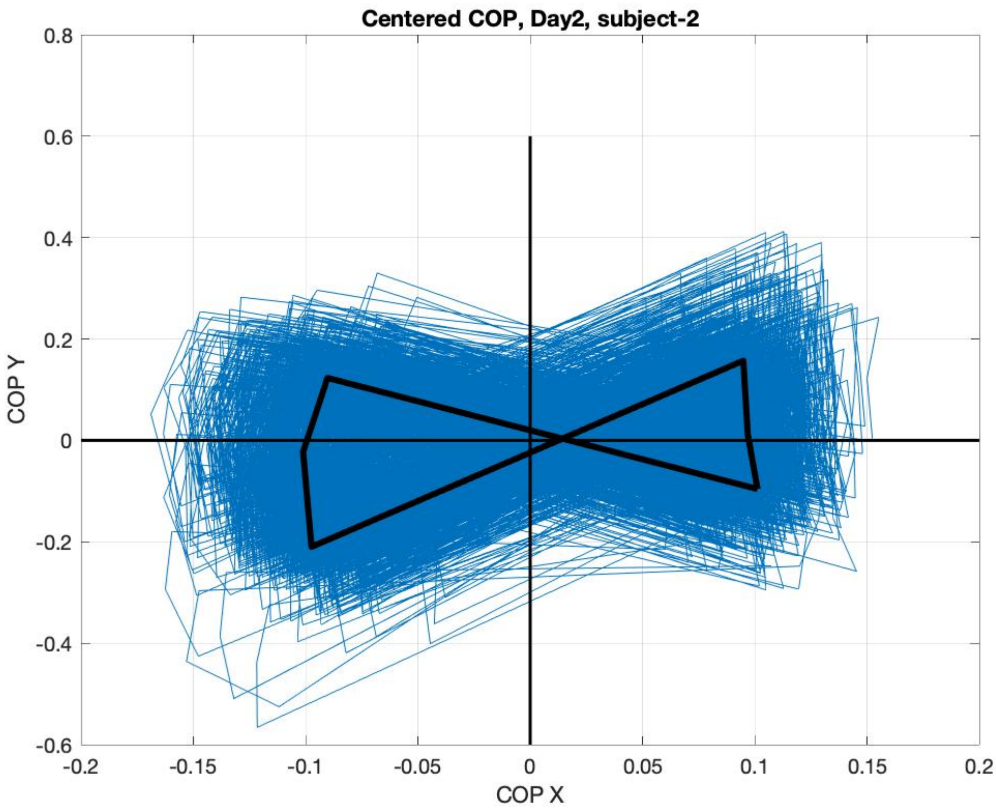
Centered COP, Day2, subject-2
0.8
0.6
0.4
0.2
0
-0.2
-0.4
-0.6
COP Y
-0.2
-0.15
-0.1
-0.05
0
0.05
0.1
0.15
0.2
COP X

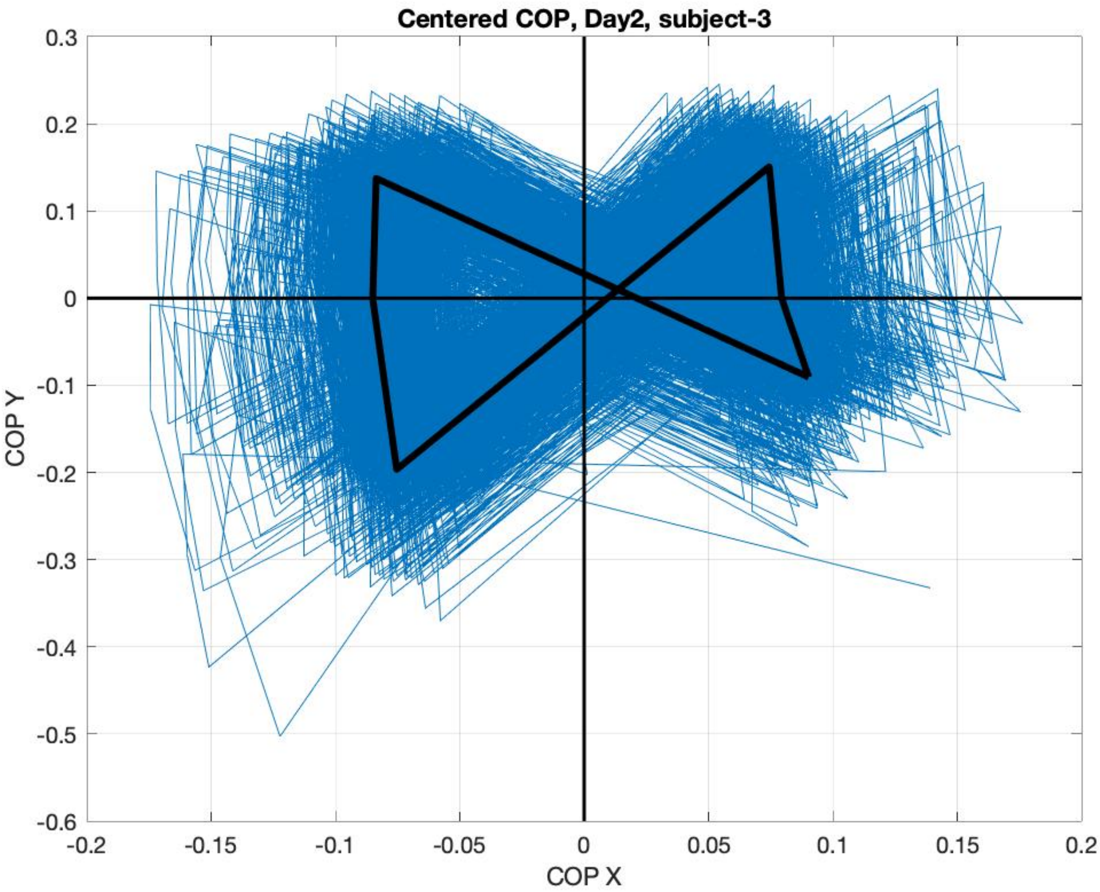
Centered COP, Day2, subject-3
COP Y
COP X
0.3
0.2
0.1
0
-0.1
-0.2
-0.3
-0.4
-0.5
-0.6
-0.2
-0.15
-0.1
-0.05
0
0.05
0.1
0.15
0.2

d)

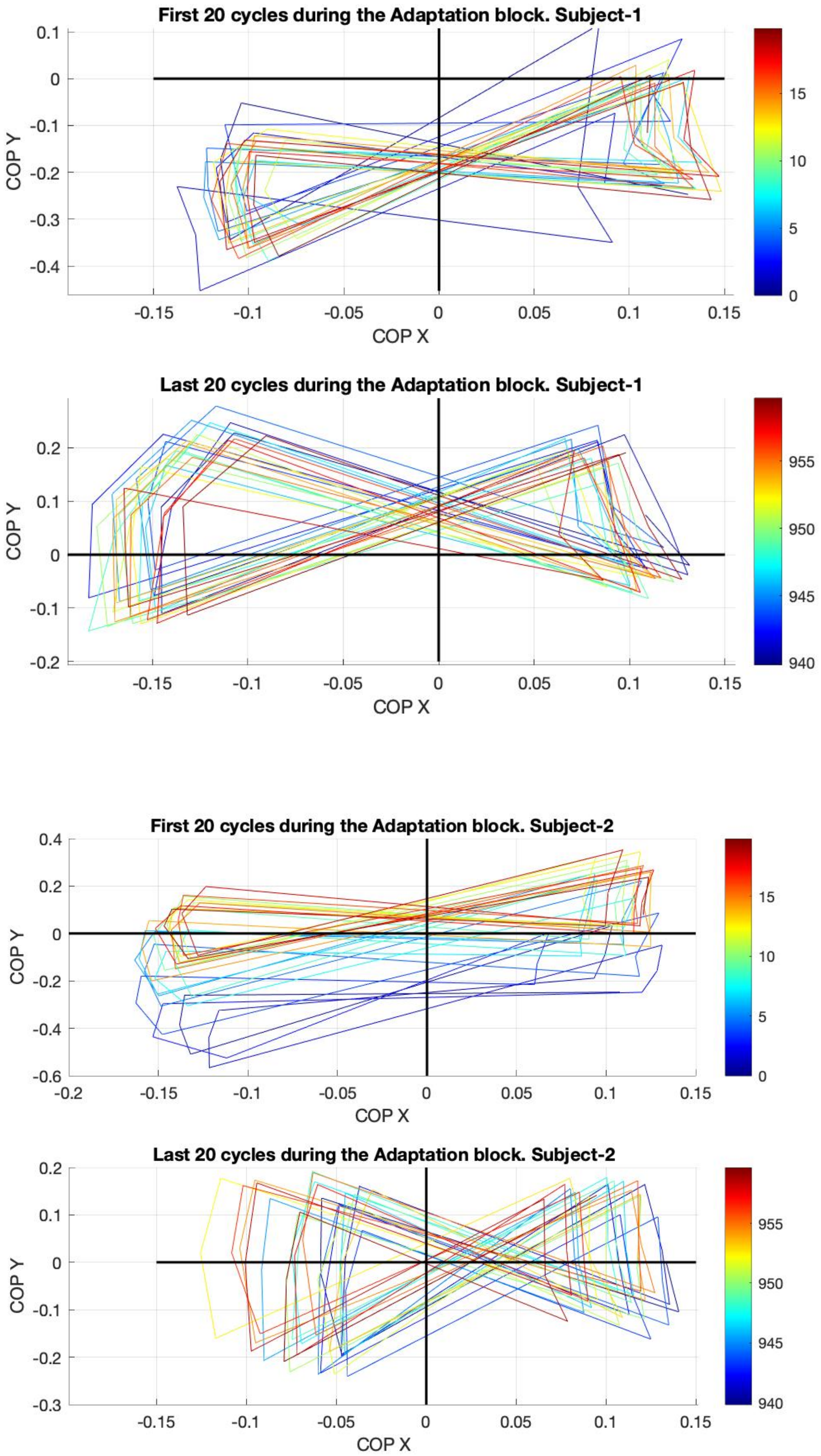
First 20 cycles during the Adaptation block. Subject-1
COP Y
COP X
0.1
0
-0.1
-0.2
-0.3
-0.4
-0.15
-0.1
-0.05
0
0.05
0.1
0.15
15
10
5
0
Last 20 cycles during the Adaptation block. Subject-1
COP Y
COP X
0.2
0.1
0
-0.1
-0.2
-0.15
-0.1
-0.05
0
0.05
0.1
0.15
955
950
945
940
First 20 cycles during the Adaptation block. Subject-2
COP Y
COP X
0.4
0.2
0
-0.2
-0.4
-0.6
-0.2
-0.15
-0.1
-0.05
0
0.05
0.1
0.15
15
10
5
0
Last 20 cycles during the Adaptation block. Subject-2
COP Y
COP X
0.2
0.1
0
-0.1
-0.2
-0.3
-0.15
-0.1
-0.05
0
0.05
0.1
0.15
955
950
945
940

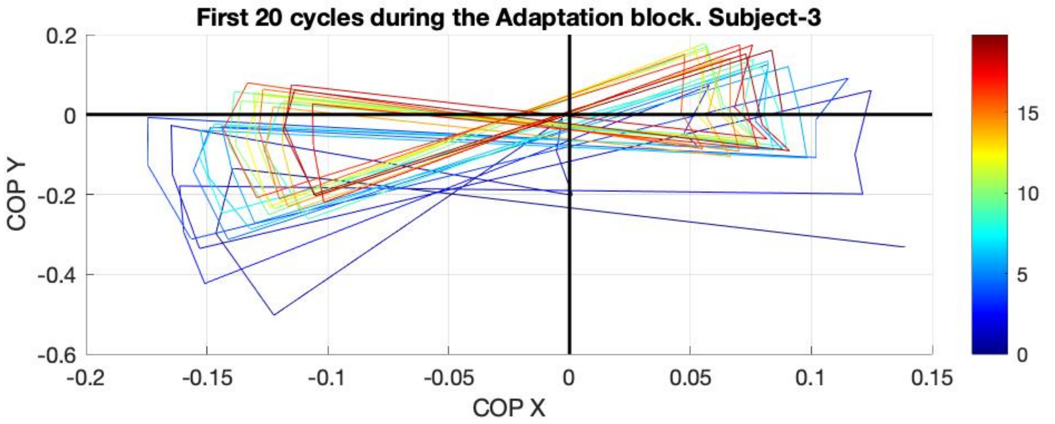

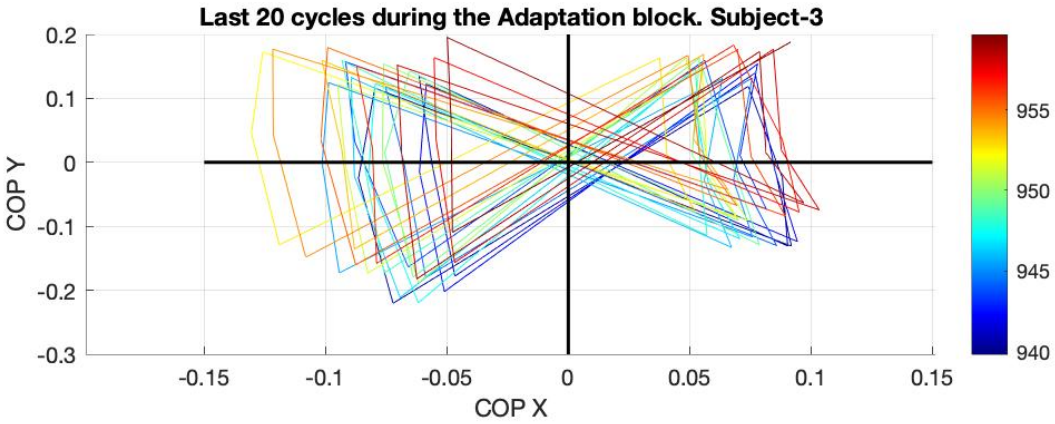

e) At the beginning of adaptation right and left wings were on different levels and there was no significant difference in their lengths. During the last cycles length of the COP butterfly became greater in fast baseline than in the slow one, but the wings were approximately on the same level.

Q3

a)

Day1:

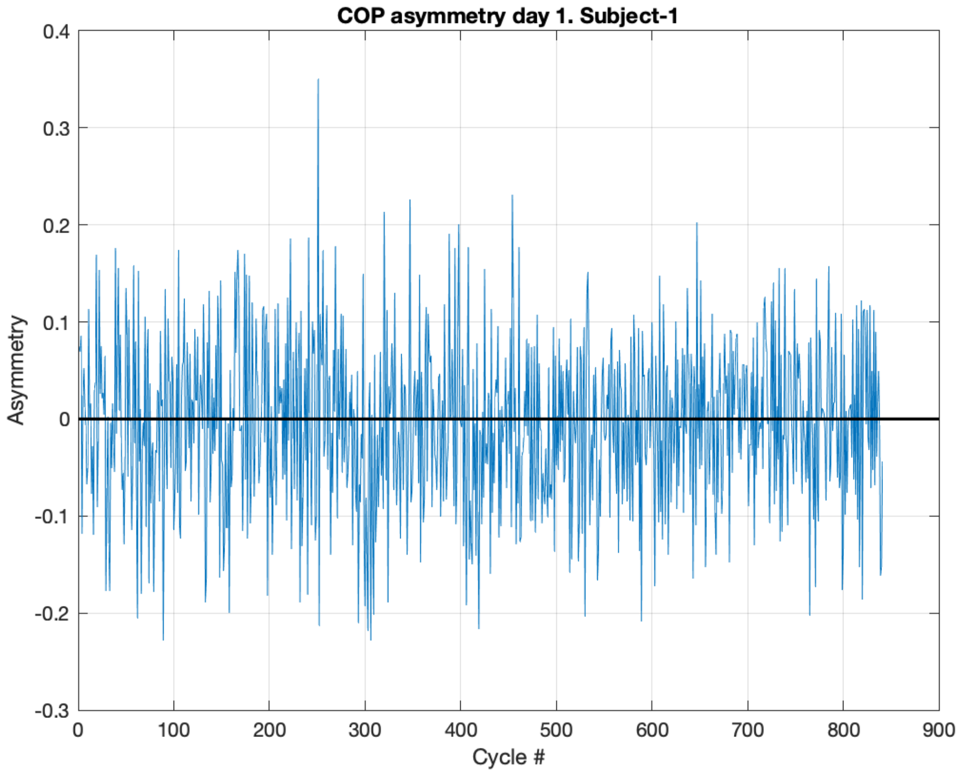
COP asymmetry day 1. Subject-1
Asymmetry
Cycle #
0.4
0.3
0.2
0.1
0
-0.1
-0.2
-0.3
0
100
200
300
400
500
600
700
800
900

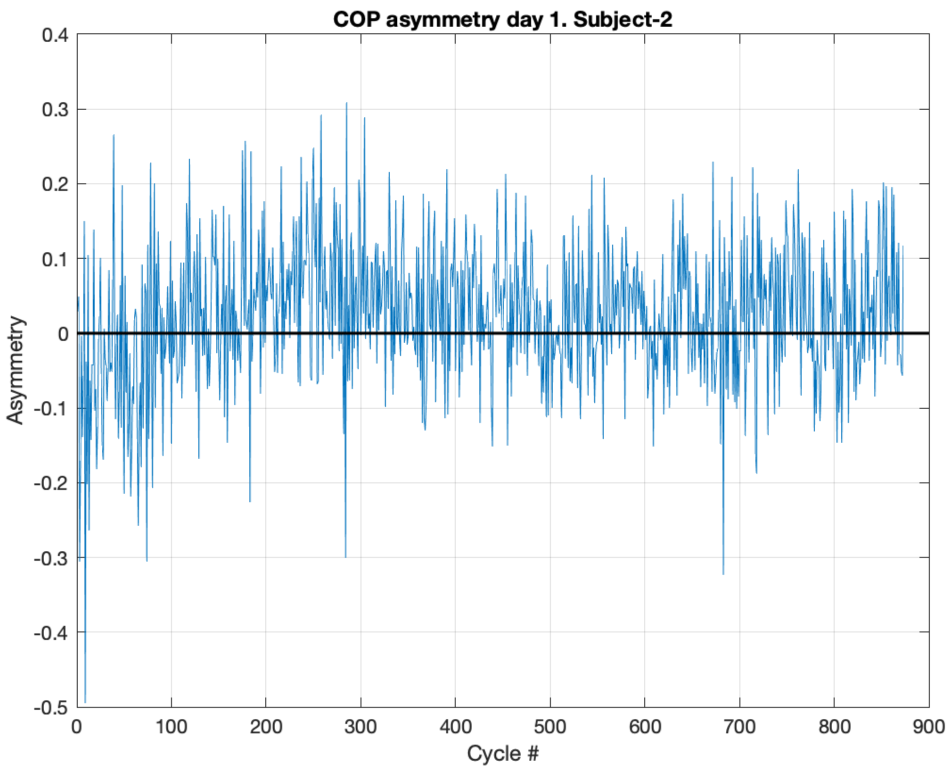
COP asymmetry day 1. Subject-2
Asymmetry
Cycle #
0.4
0.3
0.2
0.1
0
-0.1
-0.2
-0.3
-0.4
-0.5
0
100
200
300
400
500
600
700
800
900

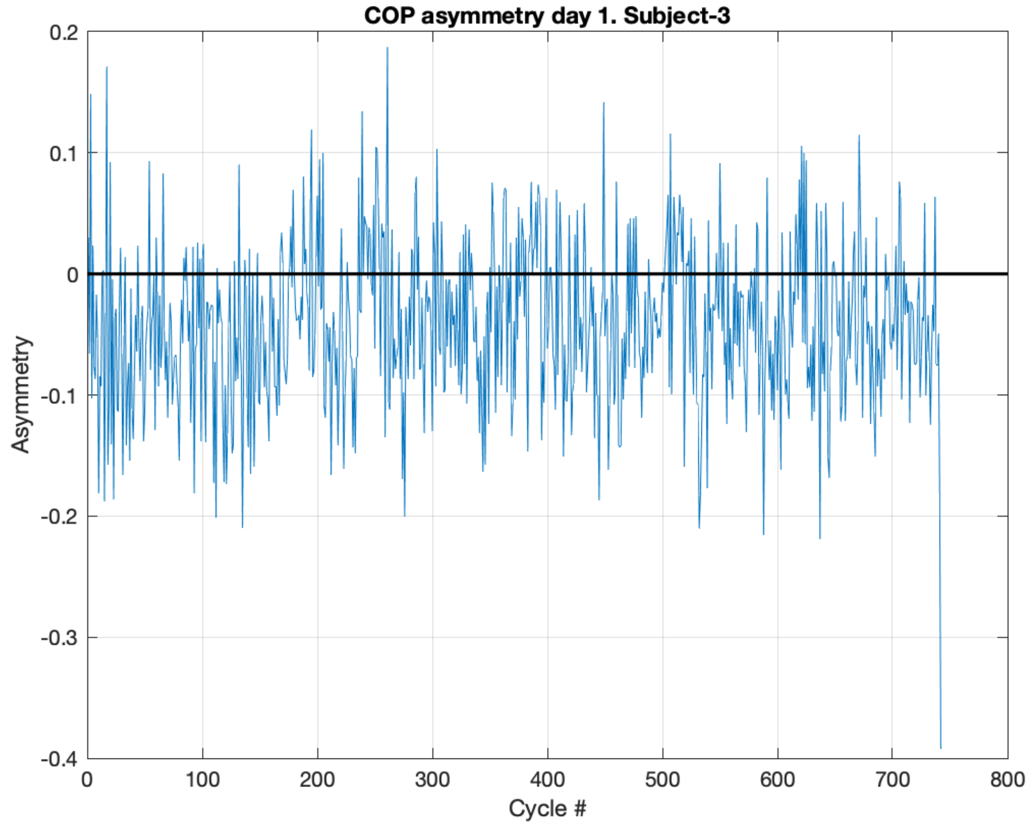
COP asymmetry day 1. Subject-3
Asymmetry
Cycle #
0.2
0.1
0
-0.1
-0.2
-0.3
-0.4
0
100
200
300
400
500
600
700
800

Day 2:

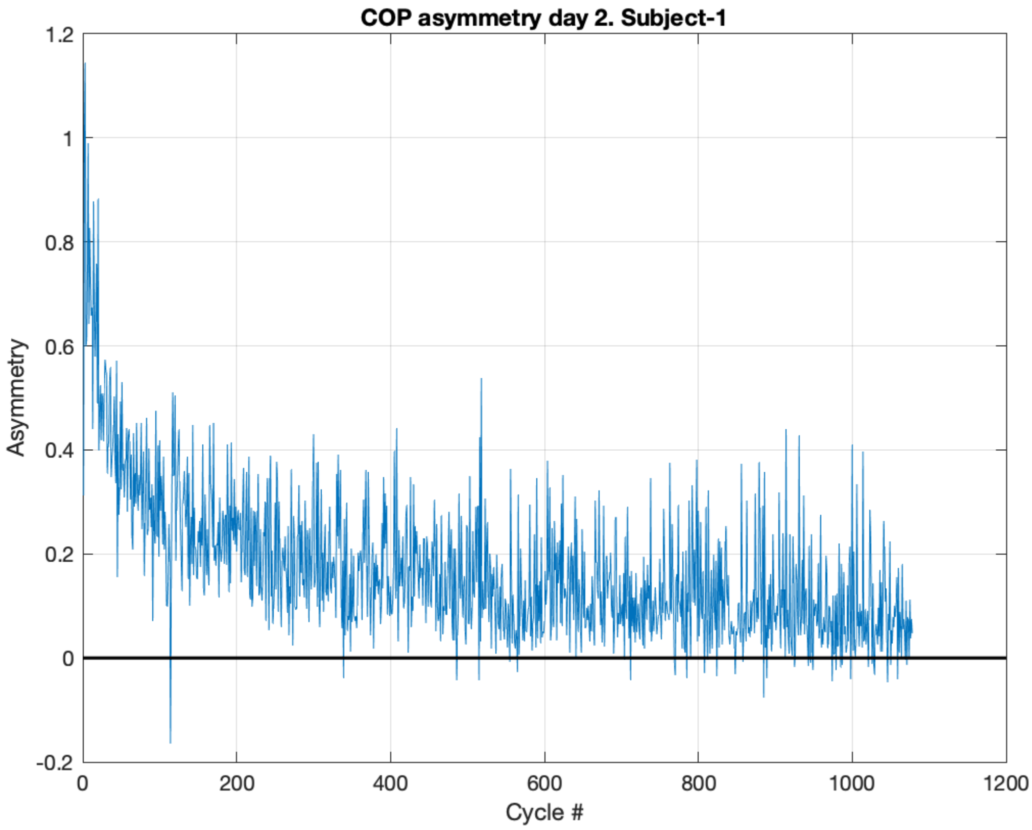
COP asymmetry day 2. Subject-1
Asymmetry
Cycle #
1.2
1
0.8
0.6
0.4
0.2
0
-0.2
0
200
400
600
800
1000
1200

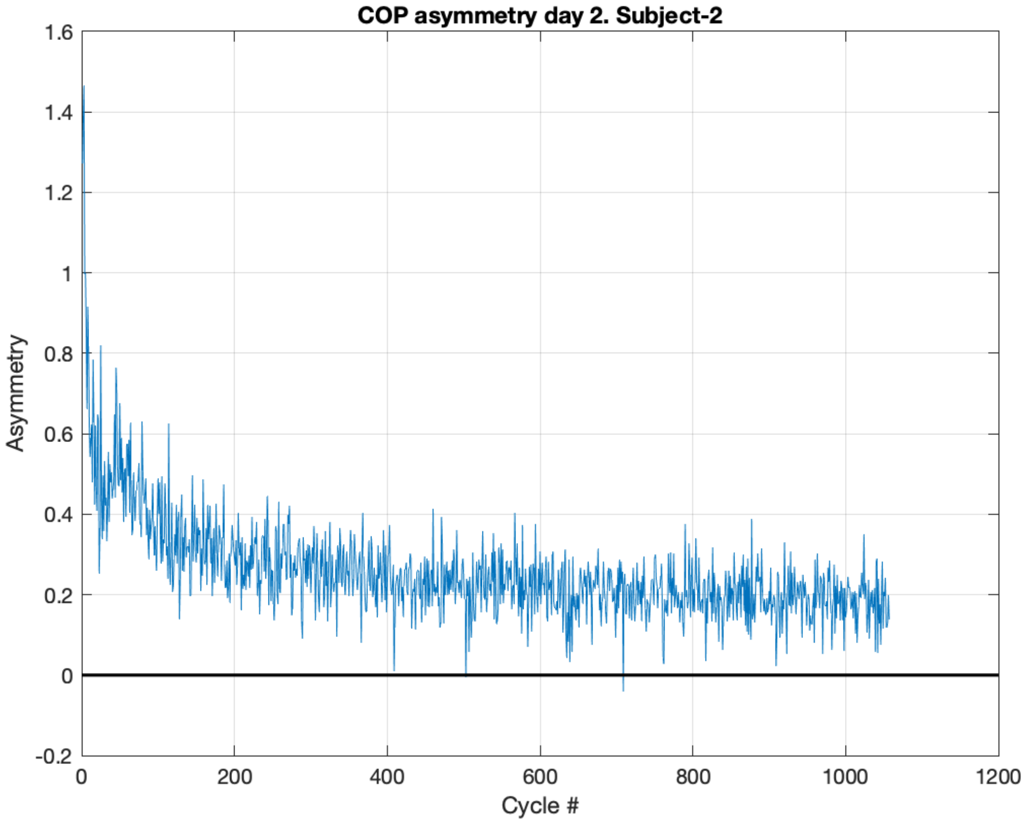
COP asymmetry day 2. Subject-2
Asymmetry
Cycle #
1.6
1.4
1.2
1
0.8
0.6
0.4
0.2
0
-0.2
0
200
400
600
800
1000
1200

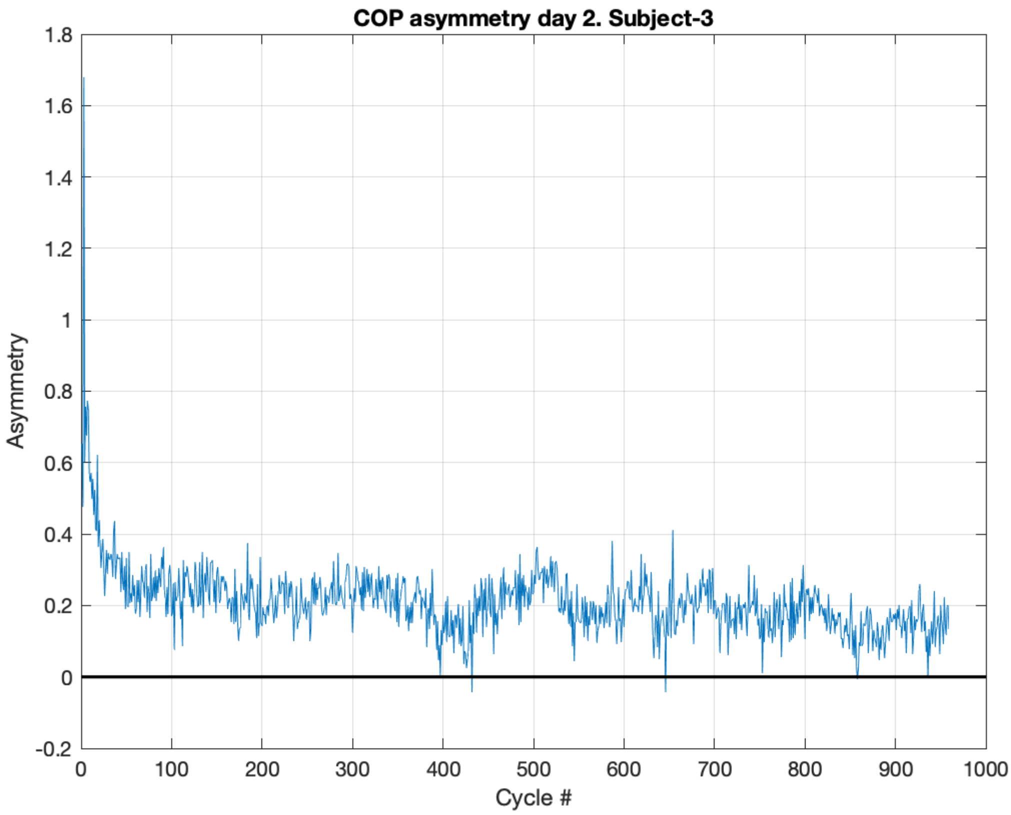
COP asymmetry day 2. Subject-3
Asymmetry
Cycle #
1.8
1.6
1.4
1.2
1
0.8
0.6
0.4
0.2
0
-0.2
0
100
200
300
400
500
600
700
800
900
1000

b) average COP asymmetry across subjects:

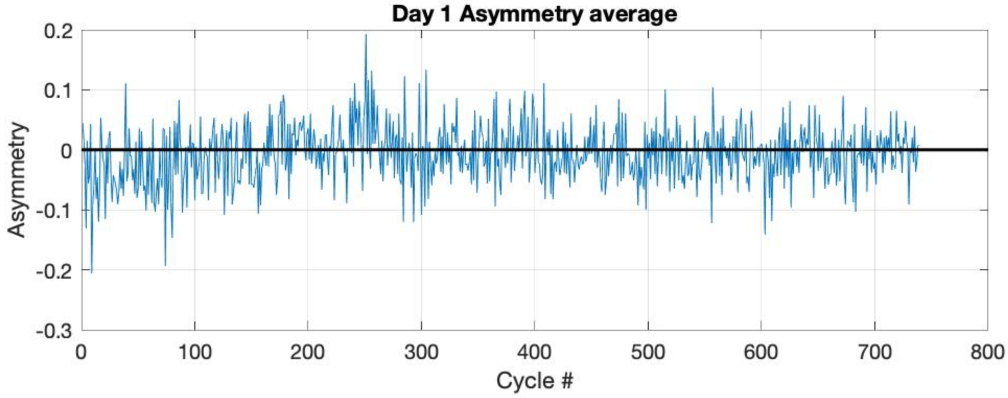

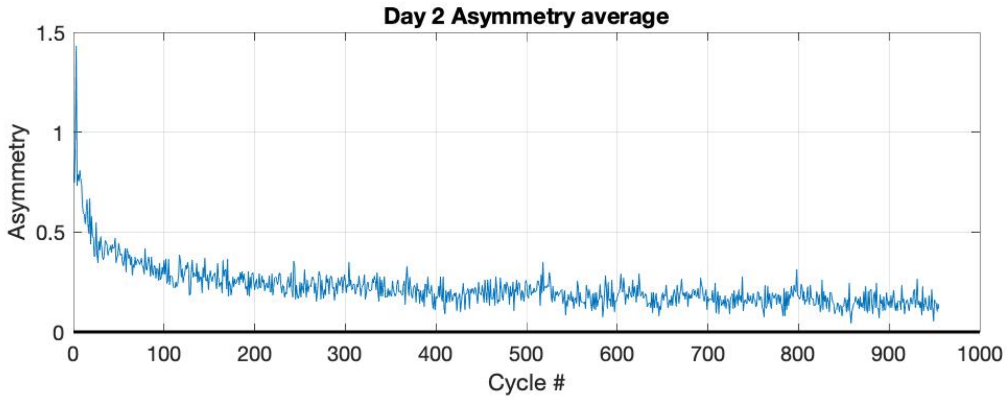

c) During the early phase the asymmetry level is the highest. During the late phase the asymmetry approaches to 0, but doesn't reach it, which means that all the subjects didn't adapt fully. Similar results were received in the literature [4].

Q4

a+b) Subject 1 Day 2

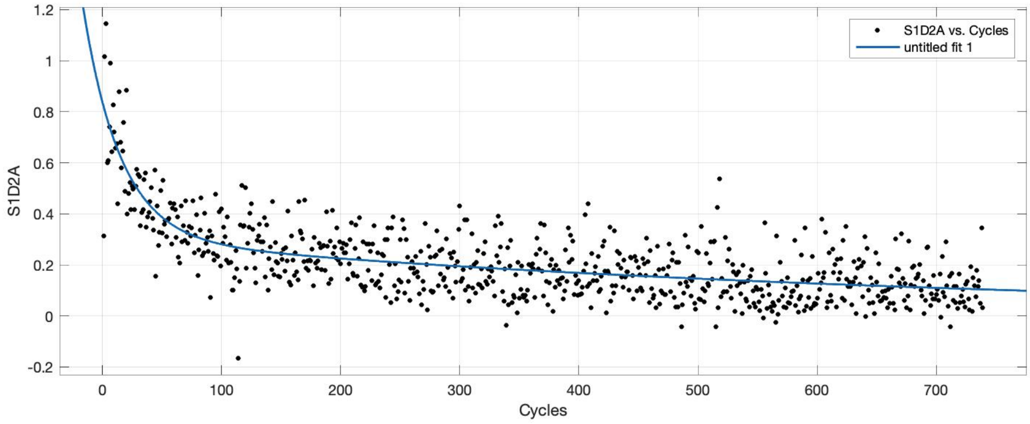

General model Exp2:
f(x) = a*exp(b*x) + c*exp(d*x)
Coefficients (with 95% confidence bounds):
a = 0.5405 (0.4689, 0.612)
b = -0.03189 (-0.03965, -0.02412)
c = 0.2979 (0.2665, 0.3293)
d = -0.001425 (-0.001698, -0.001151)

Goodness of fit:
SSE: 6.956
R-square: 0.5816
Adjusted R-square: 0.5799
RMSE: 0.09728

Subject 2 Day 2

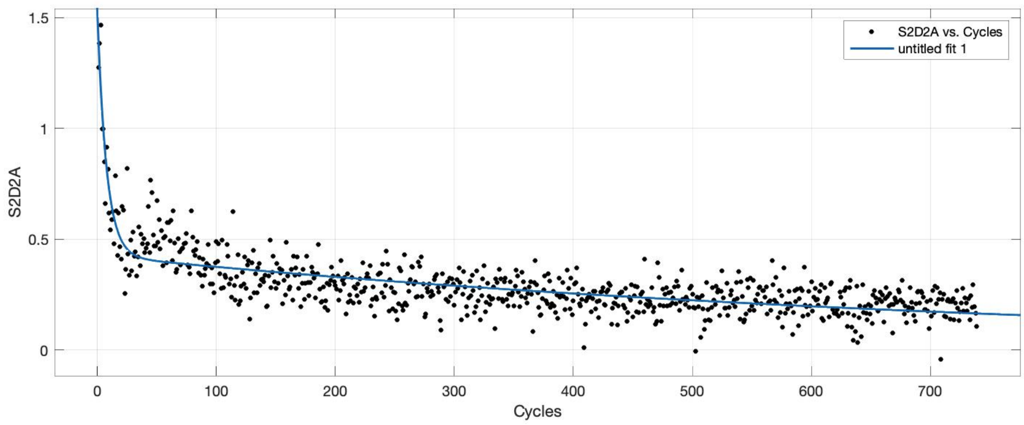

General model Exp2:
f(x) = a*exp(b*x) + c*exp(d*x)
Coefficients (with 95% confidence bounds):
a = 1.107 (0.9761, 1.239)
b = -0.1301 (-0.1519, -0.1083)
c = 0.4265 (0.41, 0.4431)
d = -0.001287 (-0.001401, -0.001173)

Goodness of fit:
SSE: 4.811
R-square: 0.6799
Adjusted R-square: 0.6786
RMSE: 0.08091

Subject 3 Day 2:

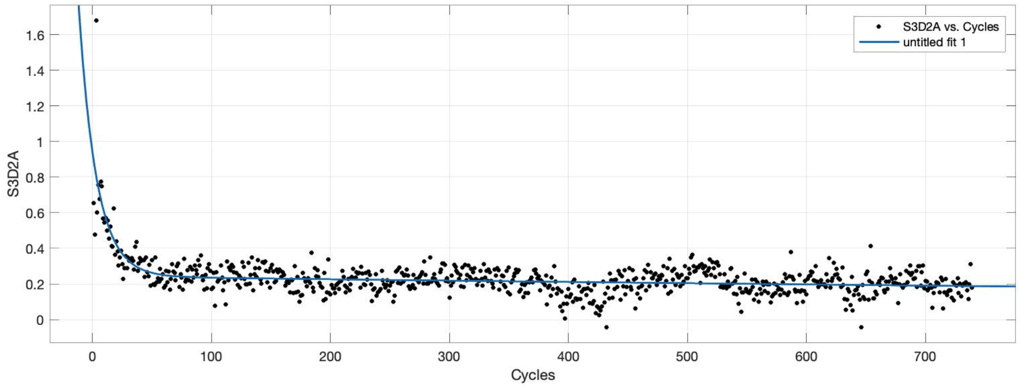

General model Exp2:
f(x) = a*exp(b*x) + c*exp(d*x)
Coefficients (with 95% confidence bounds):
a = 0.6967 (0.618, 0.7754)
b = -0.0673 (-0.07874, -0.05586)
c = 0.2426 (0.2292, 0.256)
d = -0.0003441 (-0.0004752, -0.000213)

Goodness of fit:
SSE: 3.825
R-square: 0.5085
Adjusted R-square: 0.5065
RMSE: 0.07214

For average data:

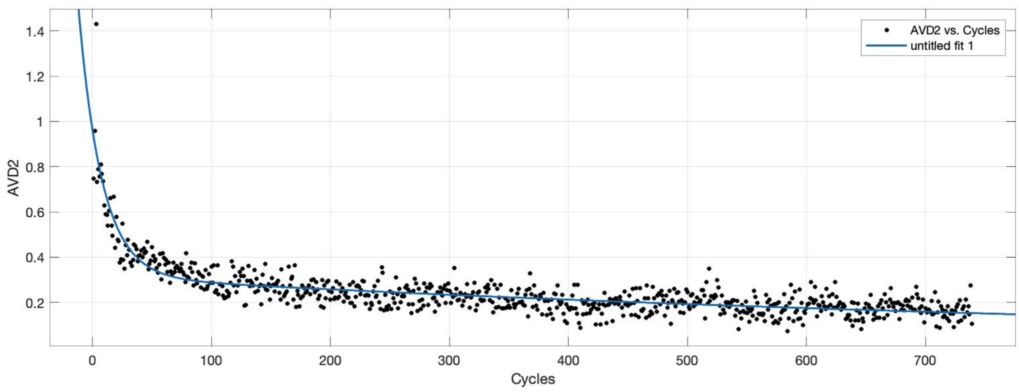

General model Exp2:
f(x) = a*exp(b*x) + c*exp(d*x)
Coefficients (with 95% confidence bounds):
a = 0.6499 (0.6025, 0.6973)
b = -0.05103 (-0.05702, -0.04504)
c = 0.3128 (0.3011, 0.3246)
d = -0.000967 (-0.001064, -0.00087)

Goodness of fit:
SSE: 1.887
R-square: 0.7946
Adjusted R-square: 0.7937
RMSE: 0.05067

c) In this part of the project we observed the ability of the human nervous system to learn and modify it's adaptation to movement.

Bibliography:

[1] J. P. Seo *et al.*, “The difference of gait pattern according to the state of the corticospinal tract in chronic hemiparetic stroke patients,” *NeuroRehabilitation*, vol. 34, no. 2, pp. 259–266, 2014.

[2] M. Whittle, *Gait Analysis: An introduction*, vol. ث قفثق, no. 2013 .ثق ثقفثق.

[3] M. M. Ardestani, M. Moazen, and Z. Jin, “Sensitivity analysis of human lower extremity joint moments due to changes in joint kinematics,” *Med. Eng. Phys.*, 2015.

[4] F. Mawase, T. Haizler, S. Bar-Haim, and A. Karniel, “Kinetic adaptation during locomotion on a split-belt treadmill,” *J. Neurophysiol.*, 2013.